

Effect of fluorine on the electrochemical properties of layered $\text{Li}(\text{Ni}_{0.5}\text{Mn}_{0.5})\text{O}_2$ cathode materials

S.-H. Kang^a, I. Belharouak^a, Y.-K. Sun^b, K. Amine^{a,*}

^a *Electrochemical Technology Program, Chemical Engineering Division, Argonne National Laboratory, Argonne, IL 60439, USA*

^b *Department of Chemical Engineering, Hanyang University, Sungdong-Gu, Seoul 133-791, South Korea*

Available online 25 May 2005

Abstract

Fluorine-doped $\text{Li}(\text{Ni}_{0.5}\text{Mn}_{0.5})\text{O}_2$ or $\text{Li}(\text{Ni}_{0.5+0.5z}\text{Mn}_{0.5-0.5z})\text{O}_{2-z}\text{F}_z$ ($0 \leq z \leq 0.2$) has been synthesized by a solid-state reaction method. X-ray diffraction patterns showed that the synthesized materials had layered $\alpha\text{-NaFeO}_2$ -type structure ($R\bar{3}m$); the Rietveld analysis revealed that lattice parameters (a and c of hexagonal setting) and degree of cation mixing increased with increasing fluorine content (z). Initial discharge capacity of the cathode materials increased with z , showed maximum at $z=0.02$, and decreased afterwards. At the same time, impedance of the cathode materials decreased with z , reached minimum at $z=0.02$, and then increased afterwards. Among the materials prepared and studied in this work, $\text{Li}(\text{Ni}_{0.51}\text{Mn}_{0.49})\text{O}_{1.98}\text{F}_{0.02}$ exhibited the best electrochemical properties in terms of capacity (151 mAh g^{-1}), impedance ($67 \Omega \text{ cm}^2$) and cycleability (no capacity fading up to 40 cycles).

© 2005 Elsevier B.V. All rights reserved.

Keywords: Li-ion battery; $\text{Li}(\text{Ni}_{0.5}\text{Mn}_{0.5})\text{O}_2$; Layered material; Fluorine substitution

1. Introduction

Recently, a lot of attention has recently been paid to layered $\text{Li}(\text{Ni}_{0.5}\text{Mn}_{0.5})\text{O}_2$ as an alternative to LiCoO_2 - and LiNiO_2 -based cathode materials for Li-ion secondary batteries [1–4]. ANL has been investigating the cathode material for high-power applications such as hybrid electric vehicles (HEVs) [2]. Due to its small amount of active nickel and a unique role of Mn^{4+} in stabilizing the structure during cycling, $\text{Li}(\text{Ni}_{0.5}\text{Mn}_{0.5})\text{O}_2$ could be a cheaper cathode material with longer cycle/calendar life and better thermal stability than $\text{Li}(\text{Ni}_{0.8}\text{Co}_{0.2})\text{O}_2$ for the HEV application. In spite of the attractive characteristics of the $\text{Li}(\text{Ni}_{0.5}\text{Mn}_{0.5})\text{O}_2$ material, however, its poor power performance prevents the material from being readily adopted in high-power battery systems [2]. ANL's strategies to improve the power performance of the $\text{Li}(\text{Ni}_{0.5}\text{Mn}_{0.5})\text{O}_2$ material have been substitution of Ni/Mn with Co and modification of particle surface with metal oxides [2,5]. In this work, the effect of

oxygen substitution with fluorine on the electrochemical properties of $\text{Li}(\text{Ni}_{0.5}\text{Mn}_{0.5})\text{O}_2$ has been investigated.

Oxygen substitution with fluorine has been reported to improve the electrochemical properties of layered $\text{Li}(\text{Ni}, \text{Co})\text{O}_2$ and LiMn_2O_4 spinel [6–10]. Kubo et al. [6,7] and Naghash and Lee [8] reported that F-substituted $\text{Li}(\text{Ni}, \text{Co})\text{O}_{2-z}\text{F}_z$ exhibited better cycle life, more stable internal impedance with cycling, and higher coulombic efficiency than unsubstituted $\text{Li}(\text{Ni}, \text{Co})\text{O}_2$ although the initial discharge capacity was sacrificed by the fluorine doping. Amatucci et al. [9,10] reported that fluorine substitution improved electrochemical properties of spinel LiMn_2O_4 , especially high temperature cycling performance. We adopted the fluorine doping strategy to improve electrochemical properties of $\text{Li}(\text{Ni}_{0.5}\text{Mn}_{0.5})\text{O}_2$, the effect of oxygen substitution with fluorine on crystal structure, electrochemical cycling performance and impedance of layered $\text{Li}(\text{Ni}_{0.5}\text{Mn}_{0.5})\text{O}_2$ is presented in this article.

2. Experimental

Fluorine-doped $\text{Li}(\text{Ni}_{0.5}\text{Mn}_{0.5})\text{O}_2$ with nominal composition of $\text{Li}(\text{Ni}_{0.5+0.5z}\text{Mn}_{0.5-0.5z})\text{O}_{2-z}\text{F}_z$ was prepared

* Corresponding author. Tel.: +1 630 252 3838; fax: +1 630 252 4176.
E-mail address: amine@cmt.anl.gov (K. Amine).

by a solid-state reaction method using Li_2CO_3 , LiF , $(\text{Ni}_x\text{Mn}_{1-x})$ -hydroxide. Oxidation states of Ni and Mn in $\text{Li}(\text{Ni}_{0.5}\text{Mn}_{0.5})\text{O}_2$ are known to be 2+ and 4+, respectively, i.e. $\text{Li}(\text{Ni}_{0.5}^{2+}\text{Mn}_{0.5}^{4+})\text{O}_2$ [2–4,11]; Ni/Mn ratio was adjusted to prevent Mn^{4+} from being reduced by the substitution of O^{2-} with F^- . Appropriate amounts of the starting materials were mixed in acetone using zirconia balls, the mixed powders were calcined at 600°C for 12 h, and then at 1000°C for 15 h in air with an intermittent grinding. Phase purity of the synthesized materials was established by powder X-ray diffraction (XRD) using Cu K α radiation.

Galvanostatic charge/discharge cycling was conducted with coin cells that were prepared in an Ar-filled glove box. The positive electrode consisted of 84 wt% metal oxide powder, 8 wt% carbon and 8 wt% polyvinylidene difluoride (PVDF) binder on aluminum foil. The negative electrode was either metallic lithium or graphite on copper foil. The electrolyte was 1 M LiPF_6 in a 1:1 mixture of ethylene carbonate (EC)/diethyl carbonate (DEC) the separator was Celgard 2500. The coin cells were galvanostatically cycled in the voltage range of 2.8–4.3 V at a current density of 0.1 mA cm^{-2} at room temperature, all of the testing were duplicated.

3. Results and discussion

In Fig. 1 are shown the XRD patterns of $\text{Li}(\text{Ni}_{0.5+0.5z}\text{Mn}_{0.5-0.5z})\text{O}_{2-z}\text{F}_z$; the diffraction patterns of the synthesized samples could be indexed based on the α - NaFeO_2 -type structure ($R\bar{3}m$). It is noted in Fig. 1 that relative intensity of (0 0 3)

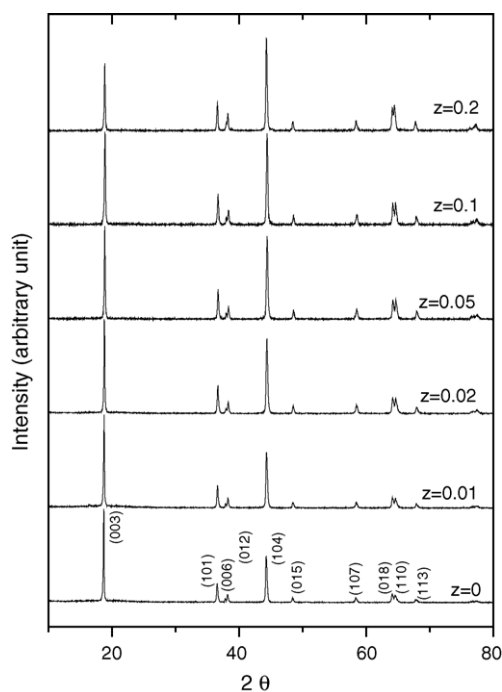


Fig. 1. XRD patterns of $\text{Li}(\text{Ni}_{0.5+0.5z}\text{Mn}_{0.5-0.5z})\text{O}_{2-z}\text{F}_z$ ($0 \leq z \leq 0.2$) calcined at 1000°C for 15 h in air.

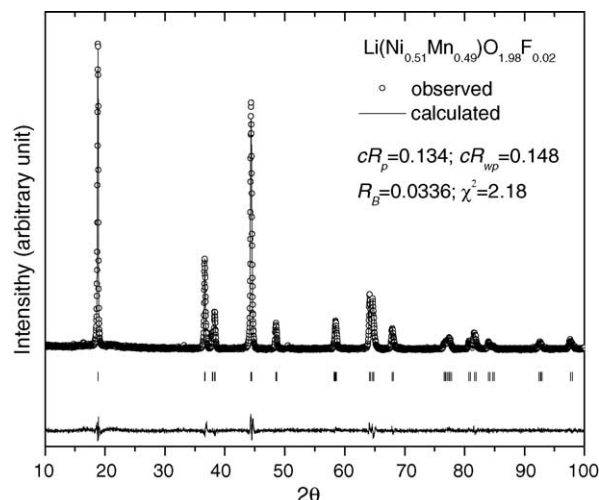


Fig. 2. The Rietveld refinement results for $\text{Li}(\text{Ni}_{0.51}\text{Mn}_{0.49})\text{O}_{1.98}\text{F}_{0.02}$.

to (1 0 4) peaks ($I_{(003)}/I_{(104)}$) decreased from 1.29 ($z=0$) to 0.607 ($z=0.2$) and splitting of (0 0 6)/(1 0 2) and (0 1 8)/(1 1 0) peaks became less clear with increasing amount of fluorine, which indicates that degree of cation disorder increases and the crystal structure becomes closer to cubic with increasing fluorine content. Naghash and Lee [12] reported the same trend in $\text{Li}_{1-z}\text{Ni}_{1+z}\text{O}_{2-y}\text{F}_y$ the intensity ratio of (0 0 3) and (1 0 4) decreased with the fluorine content. All of the XRD patterns were refined by the Rietveld analysis; an example of the Rietveld refinement is shown in Fig. 2 for the composition of $\text{Li}(\text{Ni}_{0.51}\text{Mn}_{0.49})\text{O}_{1.8}\text{F}_{0.02}$. Lattice parameters and site occupancy of all samples obtained from the Rietveld refinement are listed in Table 1. With increasing fluorine content, lattice parameters increased from $a = 2.8862\text{ \AA}$ and $c = 14.292\text{ \AA}$ for $z=0$, which are in agreement with literature values [13], to $a = 2.9000\text{ \AA}$ and $c = 14.314\text{ \AA}$ for $z=0.2$; at the same time Li occupancy in the transition metal layer (or Ni occupancy in the lithium layer) increased from 0.0585 for $z=0$ to 0.1376 for $z=0.2$, which explains the decrease of $I_{(003)}/I_{(104)}$ with increasing z . The increase of lattice parameters in spite of the replacement of O^{2-} ($r = 1.40\text{ \AA}$) with smaller F^- ($r = 1.33\text{ \AA}$) is attributed to the increase of the amount of Ni^{2+} that has larger ionic radius ($r = 0.700\text{ \AA}$) than Mn^{4+} ($r = 0.540\text{ \AA}$).

Fig. 3 shows the variation of discharge capacity of the $\text{Li}/\text{Li}(\text{Ni}_{0.5+0.5z}\text{Mn}_{0.5-0.5z})\text{O}_{2-z}\text{F}_z$ cells cycled in the voltage range of 2.8–4.3 V. The initial capacity slightly increased with fluorine substitution up to $z=0.02$, and then decreased

Table 1
Rietveld refinement results for $\text{Li}(\text{Ni}_{0.5+0.5z}\text{Mn}_{0.5-0.5z})\text{O}_{2-z}\text{F}_z$

z	a (\AA)	c (\AA)	c/a	Li(3a) or Ni(3b)
0	2.8862	14.292	4.9517	0.0585
0.01	2.8875	14.299	4.9521	0.0640
0.02	2.8889	14.304	4.9513	0.0880
0.05	2.8902	14.304	4.9491	0.1016
0.10	2.8931	14.305	4.9446	0.1096
0.20	2.9000	14.314	4.9359	0.1376

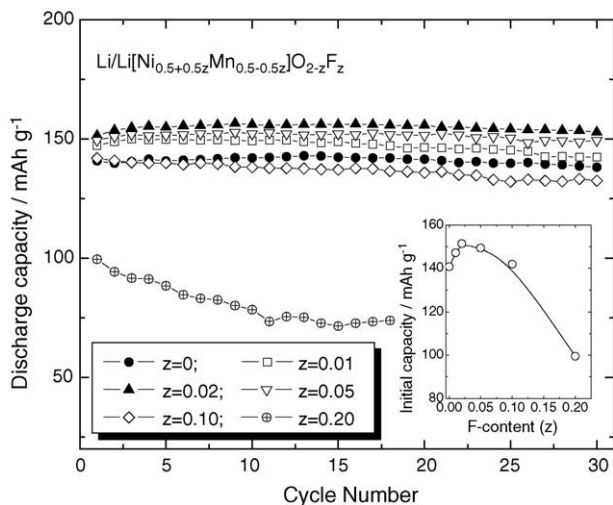


Fig. 3. Variation of discharge capacity of $\text{Li/Li}(\text{Ni}_{0.5+0.5z}\text{Mn}_{0.5-0.5z})\text{O}_{2-z}\text{F}_z$ ($0 \leq z \leq 0.2$) cells with cycling in the voltage range of 2.8–4.3 V at a current density of 0.1 mA cm^{-2} ($\sim 10 \text{ mA g}$). In the inset is shown the initial discharge capacity as a function of fluorine content.

afterwards, as is shown in the inset of Fig. 3. The cycleability was also improved slightly by the small amount of fluorine substitution. In Fig. 4 is shown the variation of area specific impedance (ASI) at 50% state-of-charge (SOC) with cycle number of $\text{C/Li}(\text{Ni}_{0.5+0.5z}\text{Mn}_{0.5-0.5z})\text{O}_{2-z}\text{F}_z$ cells. The ASI, a measure of the power performance of the Li-ion cells, was determined by $A \cdot \Delta V / I$, where A is the cross-sectional area of the electrodes, ΔV the voltage change during current interruption for 30 s at each SOC and I is the current applied during the galvanostatic cycling. As is given in the inset of Fig. 4, the initial ASI decreased significantly up to $z=0.02$ ($127 \Omega \text{ cm}^2$ for $z=0$ and $67 \Omega \text{ cm}^2$ for $z=0.02$), and then increased rapidly afterwards. As can be seen in Fig. 4, the fluorine content also affected the cycling stability of the ASI values; $\text{Li}(\text{Ni}_{0.51}\text{Mn}_{0.49})\text{O}_{1.98}\text{F}_{0.02}$ showed better cycling

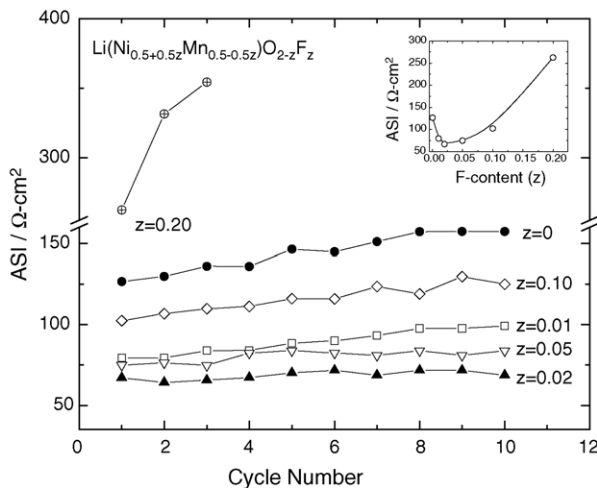


Fig. 4. Variation of ASI at 50% SOC with cycling measured with $\text{C/Li}(\text{Ni}_{0.5+0.5z}\text{Mn}_{0.5-0.5z})\text{O}_{2-z}\text{F}_z$ cells. Change of the initial ASI values at 50% SOC with fluorine content is given in the inset.

stability of ASI than other materials. The electrochemical data in Figs. 3 and 4 clearly show the beneficial effect of the fluorine substitution; $\text{Li}(\text{Ni}_{0.51}\text{Mn}_{0.49})\text{O}_{1.98}\text{F}_{0.02}$ possesses the optimum electrochemical properties among the samples studied in this work in terms of capacity, impedance and their cycleability. However, one might raise a question whether the improvement was caused solely by the fluorine doping or by the change of cationic molecular-arity (Ni/Mn ratio) as well. To answer that question, we prepared $\text{Li}(\text{Ni}_{0.51}\text{Mn}_{0.49})\text{O}_2$ via the same synthetic route as $\text{Li}(\text{Ni}_{0.51}\text{Mn}_{0.49})\text{O}_{1.98}\text{F}_{0.02}$ and compared the electrochemical properties of the two materials. Galvanostatic cycling results and area specific impedance of $\text{Li}(\text{Ni}_{0.51}\text{Mn}_{0.49})\text{O}_2$ and $\text{Li}(\text{Ni}_{0.51}\text{Mn}_{0.49})\text{O}_{1.98}\text{F}_{0.02}$ are shown in Fig. 5(a and b) together with those of $\text{Li}(\text{Ni}_{0.5}\text{Mn}_{0.5})\text{O}_2$ for comparison. $\text{Li}(\text{Ni}_{0.51}\text{Mn}_{0.49})\text{O}_2$ delivered almost the same initial capacity with $\text{Li}(\text{Ni}_{0.51}\text{Mn}_{0.49})\text{O}_{1.98}\text{F}_{0.02}$, possibly due to the increase of electrochemically active nickel content. The ASI was also lowered to some extent by the increase of the nickel content without the fluorine substitution. However, $\text{Li}(\text{Ni}_{0.51}\text{Mn}_{0.49})\text{O}_2$ exhibited poorer cycleability of capacity and ASI than $\text{Li}(\text{Ni}_{0.51}\text{Mn}_{0.49})\text{O}_{1.98}\text{F}_{0.02}$. It is not clear, at this stage, why the fluorine substituted material shows lower impedance and better cycling performance. Kubo et al. [6] attributed the lower internal impedance of $\text{Li}_{1+x}\text{Ni}_{1-x}\text{O}_{2-y}\text{F}_y$ to the weak binding of fluorine with the lattice, which gave rise to the position shifting of the ions so that the motion

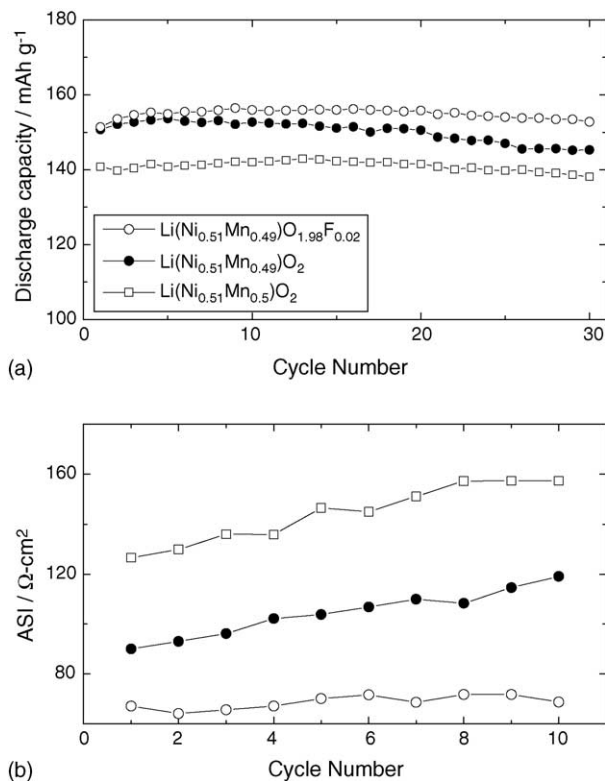


Fig. 5. Discharge capacity (a) and ASI at 50% SOC (b) of $\text{Li}(\text{Ni}_{0.5}\text{Mn}_{0.5})\text{O}_2$ and $\text{Li}(\text{Ni}_{0.51}\text{Mn}_{0.49})\text{O}_{2-z}\text{F}_z$ ($z=0, 0.02$) measured against Li metal and graphite, respectively, as a function of cycle number.

of lithium ions became easier in the crystal lattice. Nagash and Lee [8] attributed the improved cycleability and lowered overvoltage of F-substituted LiNiO_2 to suppression of Ni migration to Li sites during cycling due to the weak field of F^- ligand.

4. Summary and conclusions

Fluorine-doped $\text{Li}(\text{Ni}_{0.5}\text{Mn}_{0.5})\text{O}_2$ with a nominal composition of $\text{Li}(\text{Ni}_{0.5+0.5z}\text{Mn}_{0.5-0.5z})\text{O}_{2-z}\text{F}_z$ ($0 \leq z \leq 0.2$) was synthesized by a solid-state reaction method. The Rietveld refinement of XRD patterns of the synthesized materials showed that lattice parameters and degree of cation mixing increased with increasing fluorine content. Among the cathode materials studied in this work, $\text{Li}(\text{Ni}_{0.51}\text{Mn}_{0.49})\text{O}_{1.98}\text{F}_{0.02}$ exhibited the highest discharge capacity and the lowest impedance with the best cycling stability; $\text{Li}(\text{Ni}_{0.51}\text{Mn}_{0.49})\text{O}_{1.98}\text{F}_{0.02}$ delivered stable discharge capacity of 151 mAh g^{-1} at 2.8–4.3 V and exhibited ASI value of $67 \Omega \text{ cm}^2$ at 50% SOC whereas those of $\text{Li}(\text{Ni}_{0.5}\text{Mn}_{0.5})\text{O}_2$ were 141 mAh g^{-1} and $127 \Omega \text{ cm}^2$, respectively. From the experimental results shown in this work, it is concluded that fluorine substitution is an effective way in increasing capacity and lowering impedance as well as in improving the cycling performance of the $\text{Li}(\text{Ni}_{0.5}\text{Mn}_{0.5})\text{O}_2$ material.

Acknowledgments

The authors acknowledge the financial support of the U.S. Department of Energy, FreedomCAR and Vehicle Technologies Program, under Contract No. W-31-109-Eng-38.

References

- [1] T. Ohzuku, Y. Makimura, *Chem. Lett.* 30 (2001) 744.
- [2] S.-H. Kang, J. Kim, M.E. Stoll, D.A. Abraham, Y.-K. Sun, K. Amine, *J. Power Sources* 112 (2002) 41.
- [3] J.-S. Kim, C.S. Johnson, M.M. Thackeray, *Electrochem. Commun.* 4 (2002) 205.
- [4] W.-S. Yoon, Y. Paik, X.-Q. Yang, M. Balasubramanian, J. McBreen, C.P. Grey, *Electrochem. Solid-State Lett.* 5 (2002) 263.
- [5] S.-H. Kang, S.Y. Yoon, K. Amine, 204th ECS Meeting, Orlando, FL, October 12–17, 2003 (Abstract No. 259).
- [6] K. Kubo, M. Fujiwara, S. Yamada, S. Arai, M. Kanda, *J. Power Sources* 68 (1997) 553.
- [7] K. Kubo, S. Arai, S. Yamada, M. Kanda, *J. Power Sources* 81 (1999) 599.
- [8] A.R. Naghash, J.Y. Lee, *Electrochim. Acta* 46 (2001) 2293.
- [9] G.G. Amatucci, N. Pereira, T. Zheng, I. Plitz, J.-M. Tarascon, *J. Power Sources* 81 (1999) 39.
- [10] G.G. Amatucci, N. Pereira, T. Zheng, J.-M. Tarascon, *J. Electrochem. Soc.* 148 (2001) 171.
- [11] J. Reed, G. Ceder, *Electrochem. Solid-State Lett.* 5 (2002) 145.
- [12] A.R. Naghash, J.Y. Lee, *Electrochim. Acta* 46 (2001) 941.
- [13] Y. Makimura, T. Ohzuku, *J. Power Sources* 119 (2003) 156.